VOL. 77, NO. 26 JOURNAL OF GEOPHYSICAL RESEARCH SEPTEMBER 10, 1972

Equations of State and Phase Equilibria of Stishovite and a Coesitelike Phase from Shock-Wave and Other Data[1]

GEOFFREY F. DAVIES

Seismological Laboratory, California Institute of Technology, Pasadena, California 91109

Shock-wave, static-compression (X ray), ultrasonic, thermal expansion, and thermodynamic data are simultaneously inverted to determine the equations of state of stishovite and a coesitelike SiO_2 phase. All the stishovite data except the thermal expansion data are satisfied by a Mie-Grüneisen–type equation of state having a zero pressure bulk modulus K of about 3.50 ± 0.1 Mb, a pressure derivative dK/dP of 3.3 ± 1, and a Grüneisen parameter, initially 1.25 ± 0.1, that decreases slowly with compression. The volume coefficient of thermal expansion at ambient conditions is found to be $13 \pm 1 \times 10^{-6}$/°K, in comparison with 16.4 ± 1.3 measured by Weaver. Some Hugoniot data of Trunin et al. for very porous quartz have densities very close to the density of coesite. However, a calculation of the coesite-stishovite phase line shows that the coesitelike phase persists to about twice the predicted transition pressure at 10,000°K. It is suggested that the discrepancy can be explained if this phase is interpreted as a liquid of about coesite density.

Since the discovery of the dense high-pressure silica polymorph stishovite [*Stishov and Popova*, 1961] and its subsequent identification both in natural silica from a meteor crater [*Chao et al.*, 1962] and as the dense phase obtained in the shock-wave experiments of *Wackerle* [1962] by *McQueen et al.* [1963], a variety of experiments have yielded considerable data on stishovite. To date, these data include more shock-wave, static-compression (X ray), thermodynamic, thermal expansion, and, very recently, ultrasonic data. These data, with their sources and other relevant information, are summarized in Table 1. A succession of analyses of these data has accompanied their accumulation [*Anderson and Kanamori*, 1968; *Ahrens et al.*, 1969, 1970]. This paper is another in that succession.

The Grüneisen parameter γ is an important quantity that characterizes thermal effects in the equation of state. *Ahrens et al.* [1970], returning to the method used by *McQueen et al.* [1963], determined the values of γ at large compression from the difference in pressure between Hugoniots corresponding to different initial densities. This method is preferable to that used by *Anderson and Kanamori* [1968] and *Ahrens et al.* [1969], who used the *Slater* [1939] or *Dugdale and MacDonald* [1953] formulas for the volume dependence of γ. These formulas have been severely criticized because they fail to take account of the frequently large pressure dependence of the shear modes of vibration [*Knopoff and Shapiro*, 1969].

Fitting these results with the functional form

$$\gamma = \gamma_0(V/V_0)^A \qquad (1)$$

where V is the specific volume, A is a constant, and the subscript 0 denotes zero pressure, *Ahrens et al.* [1970] adjusted γ_0 until the volume coefficient of thermal expansion α, obtained from the identity

$$\alpha = \gamma\rho C_p/K_s \qquad (2)$$

where K_s is determined from the shock-wave analysis, agreed with the measured value. (The value used was the preliminary value of $\alpha = 15 \times 10^{-6}$/°K, obtained from J. S. Weaver (personal communication, 1969), cf. Table 1.) In (2), K_s is the isentropic bulk modulus, ρ is the density, and C_p is the specific heat at constant pressure.

Since that analysis, several new sets of data have been published. The data of *Trunin et al.* [1971*a*] greatly extend the pressure range of the Hugoniot data, and those of *Trunin et al.* [1971*b*] extend the range of initial porosities.

[1] Contribution 2101, Division of Geological and Planetary Sciences, California Institute of Technology.

TABLE 1*a*. Shock-Wave and Static-Compression Data for Stishovite

Code	Source	No. of Points	Initial Density, g/cm^3	Pressure Range, Mb
	Shock-Wave Data			
S1	*Wackerle* [1962]	12	2.65	0.4 to 0.7
S2	*Al'tshuler et al.* [1965]	3	2.65	0.6 to 2.0
S3	*Trunin et al.* [1971*a*]	12	2.65	0.4 to 6.5
S4	*Wackerle* [1962]	3	2.20	0.5 to 0.6
S5	H. Shipman (private communication, 1969)	5	2.20	0.6 to 1.6
S6	*McQueen* [1968]	34	2.20	0.4 to 0.8
S7	*Trunin et al.* [1971*b*]	2	2.20	0.5 to 1.6
S8	*Jones et al.* [1968]	6	1.98	0.4 to 1.4
S9	*Trunin et al.* [1971*b*]	6	1.77	0.2 to 2.3
S10	*Trunin et al.* [1971*b*]	3*	1.55	0.3 to 0.6
	Static-Compression Data			
X1	*Liu et al.* [1972]	9		0 to 223†
X2	*Bassett and Barnett* [1970]	14		0 to 85†

*May be interpreted as coesite-stishovite mixture (see text).
†Value in kilobars.

The resultant wide spread of the Hugoniots provides stronger constraints on γ. Also, *Mizutani et al.* [1972] have measured ultrasonically the compressional- and shear-wave velocities of stishovite, and thus another constraint on K_s is provided.

In addition to benefiting from the newly available data and using a different form of the equation of state (discussed below), the present analysis determines simultaneously the compressional and thermal parts of the equation of state by adjusting simultaneously all free parameters to give a least-squares fit to all the data. This procedure accomplishes implicitly the two sequential stages of the analysis of *Ahrens et al.* [1970].

Trunin et al. [1971*b*] noted that the Hugoniots of their most porous quartz samples achieved densities significantly less than the density of stishovite and that they extrapolated approximately to the zero pressure density of coesite. On this basis they identified these Hugoniots as representing the coesite phase. Although coesite is stable at room temperature in the approximate pressure range 30–70 kb between the stability fields of quartz and stishovite, coesite has not previously been observed in shock-wave experiments, the transformation usually being directly from quartz to stishovite. There are enough other coesite data (Table 2) that, when they are combined with these Hugoniot data and when it is assumed that they do

TABLE 1*b*. Other Data for Stishovite

Source	Quantity	Value
Mizutani et al. [1972]	Compressional-wave velocity	V_p = 11.0 km/sec
	Shear-wave velocity	V_s = 5.50 km/sec
	Isentropic bulk modulus	K_s = 3.46 ± 0.24 Mb
Weaver [1971]	Volume coefficient of thermal expansion (300°K)	α = 16.4 ± 1.3/°K
Holm et al. [1967]	Specific heat at constant pressure (300°K)	C_p = 7.15 x 10^6 ergs/g °K
Kieffer and Kamb [1972]	High temperature limit of Debye temperature	θ_D ~ 1120°K
Robie et al. [1966]	Density, zero pressure, 298°K	ρ_0 = 4.287 g/cm^3

TABLE 2*a*. Shock-Wave and Static-Compression Data for Coesite

Code	Source	No. of Points	Initial Density, g/cm^3	Pressure Range, kb
		Shock-Wave Data		
S11	*Trunin et al.* [1971*b*]	3	1.35	119 to 322
S12	*Trunin et al.* [1971*b*]	2	1.35	454 to 552
S13	*Trunin et al.* [1971*b*]	5	1.15	65 to 477
		Static-Compression Data		
X3	*Bassett and Barnett* [1970]	11		0 to 80

indeed represent coesite, the equation of state can be approximately determined. The success of this procedure seems to support the coesite identification, but other calculations suggest otherwise, as will be seen.

Trunin et al. [1971*b*] also calculated approximate Hugoniot temperatures and suggested that the boundary separating the coesite and stishovite fields in a pressure-temperature plot represented the coesite-stishovite phase transition line. Hugoniot temperatures have been recalculated here, and, in addition, the coesite-stishovite phase line has been independently calculated from the equations of state of the two phases, the coesite identification again being assumed. There is a large discrepancy between the two approaches. It is suggested that the new phase may in fact be a liquid of approximately the density of coesite rather than coesite itself. Because some of the properties of this liquid are unknown, it is necessary to proceed as if the phase were solid coesite and to examine the plausibility of the results.

ANALYSIS

A complete equation of state must account for both compressional and thermal effects. Previous studies have accounted for these effects by invoking the Mie-Grüneisen equation, incorporating a finite strain description of compressional effects with various expressions for the Grüneisen parameter to describe thermal effects, as was discussed in the introduction. The problem is to find an expression for γ that does not involve overrestrictive assumptions and that has some theoretical foundation.

Thomsen [1970] has considered the question of incorporating the results of the theory of anharmonic lattice dynamics into finite strain

TABLE 2*b*. Other Data for Coesite

Source	Quantity	Value
Skinner [1966]	Volume coefficient of thermal expansion (293°K)	$\alpha = 8.0 \times 10^{-6}$/°K
Holm et al. [1967]	Specific heat at constant pressure (300°K)	$C_p = 7.46 \times 10^6$ ergs/°K
Kieffer and Kamb [1972]	High temperature limit of Debye temperature	$\theta_D \approx 1170$°K
Robie et al. [1966]	Density, zero pressure, 298°K	$\rho_0 = 2.91$ g/cm^3
Mizutani et al. [1972]	Compressional-wave velocity Shear-wave velocity Isentropic bulk modulus	$V_p = 7.53$ km/sec $V_s = 4.19$ km/sec $K_s = 0.97$ Mb

theory. Lattice dynamics in the fourth-order approximation lead, under certain assumptions, to the Mie-Grüneisen equation [*Leibfried and Ludwig*, 1961], and *Thomsen* [1970] derived an expansion of this equation into the domain of finite strain. His equation thus describes both compressional and thermal effects. It is written in terms of a particular Lagrangian strain and involves six adjustable parameters. Subsequently it has been shown (G. F. Davies, unpublished manuscript, 1972) that analogous equations can be derived in terms of other strains and that the resulting form of the Mie-Grüneisen equation can be written in the form of a conventional finite strain equation.

In accord with these results, the 300°K isotherm will be represented in this study by the fourth-order Eulerian finite strain equation

$$P(V) = -3K_0(1 - 2\epsilon)^{5/2}\{\epsilon - \tfrac{3}{2}(K_0' - 4)\epsilon^2 + \tfrac{3}{2}[K_0K_0'' + K_0'(K_0' - 7) + \tfrac{143}{9}]\epsilon^3\} \quad (3)$$

where K_0 is the bulk modulus at zero pressure and 300°K, a prime denotes an isothermal pressure derivative, and

$$\epsilon = \tfrac{1}{2}[1 - (V/V_0)^{-2/3}] \quad (4)$$

is the Eulerian strain parameter. Neglecting the last term in (3) reduces it to the familiar Birch-Murnaghan equation [e.g., *Birch*, 1952].

The particular expression for γ to be used here is derived (G. F. Davies, unpublished manuscript, 1972) by expanding to second order the squared eigenfrequencies of the lattice in terms of displacements of the atoms from their mean lattice positions and substituting the result in the usual definition of γ:

$$\gamma = -\frac{d \ln \omega}{d \ln V} = -\frac{(1 + e)(g + he)}{6(1 + ge + \tfrac{1}{2}he^2)} \quad (5)$$

Here e is another strain parameter defined as

$$e = (V/V_0)^{1/3} - 1 \quad (6)$$

The strain e is linear in atomic displacements, so that a second-order expansion in terms of e is identical to a second-order expansion in terms of atomic displacements. This result, in turn, is consistent with the expansion of the lattice potential energy to fourth order in terms of atomic displacements on which the fourth-order theory of lattice dynamics is based [*Leibfried and Ludwig*, 1961]. The quantity ω in (5) can be regarded as a characteristic eigenfrequency of the lattice.

The constants g and h in (5) are parameters to be determined. They are related to measured quantities by the following series of equations (G. F. Davies, unpublished manuscript, 1972).

$$g = -6\gamma_0 \quad (7)$$

$$h = g\left[3\left(\frac{\partial \ln \gamma}{\partial \ln V}\right)_{T,O} + g - 1\right] \quad (8)$$

$$\gamma = V\alpha K_T/C_v \quad (9)$$

$$\left(\frac{\partial \ln \gamma}{\partial \ln V}\right)_T = 1 + \delta_T - K_T' - \left(\frac{\partial \ln C_v}{\partial \ln V}\right)_T \quad (10)$$

$$\delta_T = -|/\alpha K_T|(\partial K_T/\partial T)_P \quad (11)$$

Here C_v is the specific heat at constant volume and the subscript T denotes isothermal derivatives. Equations 9 and 10 are thermodynamic identities [*Bassett et al.*, 1968].

An equation for Hugoniot pressure can be derived by combining the Mie-Grüneisen equation with the Rankine-Hugoniot conservation equations. In this way the Hugoniot pressure can be related to any other thermodynamic locus, such as an isentrope or an isotherm. An equation relating the Hugoniot pressure to an isentrope has been given by *Ahrens et al.* [1969]. Another equation relating Hugoniot pressure to the isotherm of the static lattice has been given by *Thomsen* [1970]. This equation has been generalized to include the effects of a phase change and initial porosity (G. F. Davies, unpublished manuscript, 1972); the result is

$$P_h\left(\frac{V_0'}{2} - \frac{V}{2} - \frac{V}{\gamma}\right) = \phi(V) - \phi(V_0) + \frac{V}{\gamma}\frac{d\phi}{dV} - U(V_0) + E_t \quad (12)$$

where P_h is the Hugoniot pressure, V_0' is the initial density of the sample, V_0 is the zero pressure density of the phase in question, U is the thermal energy, E_t is the zero pressure phase transformation energy, and ϕ is the potential energy of the static lattice. The quan-

tity ϕ can be related to the expansion of the isotherm (equation 3) through the constants g and h (G. F. Davies, unpublished manuscript, 1972).

To summarize, expressions for the 300°K isotherm and for the Hugoniots are given by (3) and (12) in terms of the six parameters V_0, K_0, K_0', K_0'', g, and h. The only essentially new thing in this analysis is the equation for γ (equation 5). It should be noted that this equation gives a volume dependence of γ qualitatively similar to, for instance, (1). In the present application the volume dependence of γ is constrained by the Hugoniot data, and so the quantitative differences between (1) and (5), for instance, will be absorbed by their parameters. Thus with (5) the value of δ_T will be determined in this way (see equations 10 and 11; all other quantities in (7)–(11) are constrained by other aspects of the data). Because δ_T is otherwise unknown, the only doubt resulting from this procedure concerns the specific value of δ_T.

The specific heat at constant volume has been approximated in these calculations by the Debye model. A discussion of the inadequacy of the Debye model for a number of minerals has been given by *Kieffer and Kamb* [1972]. Their results indicate that, for the purposes of this discussion, the Debye model is not too inadequate for stishovite. It is less appropriate for coesite, but, in view of the other uncertainties of the coesite equation of state (see below), it is an acceptable approximation.

Hugoniot temperatures are calculated according to a method given by *Ahrens et al.* [1969]. For this calculation the volume dependence of the Debye temperature θ_D is required. The Debye temperature is proportional to the Debye cutoff frequency. Thus, for consistency with the treatment of lattice dynamics discussed earlier, the square of θ_D may be expanded to second order in e. Thus

$$\theta_D(V) = \theta_D(V_0)(1 + ge + \tfrac{1}{2}he^2)^{1/2} \qquad (13)$$

EQUATIONS OF STATE

General. The procedure used here to determine the equation of state was to calculate, according to the last section, all relevant quantities, such as Hugoniots, isotherms, bulk modulus, and so forth, and to adjust the equation-of-state parameters to obtain a weighted least-squares fit to the data. The weighting basically was done according to the estimated standard error of the data, but it was also adjusted in some cases, as will be seen, to preferentially fit some of the data.

Some general features of the silica Hugoniot data and a representative set of calculated Hugoniots and isotherms are illustrated in Figure 1. Most of the Hugoniot data radiate from one of two points: the coesite or sitishovite zero pressure densities. The apparent zero pressure density of the data is the basis of the identification by *Trunin et al.* [1971*b*] of the Hugoniots of the two most porous silica samples as being in the coesite phase. This identification will be discussed subsequently; in the meantime the phase will be referred to as 'coesite.'

The Hugoniots of successively more porous silica, which start at zero porosity, become successively steeper up to the initial density ρ_0' of 1.77 g/cm^3, whose Hugoniot is nearly vertical on this plot. The 1.55-g/cm^3 initial density Hugoniot data are at densities lower than but fairly close to the zero pressure 300°K stishovite density, whereas the 1.35- and 1.15-g/cm^3 initial density Hugoniots are less steep and centered about the coesite density. The $\rho_0' = 1.55$ g/cm^3 Hugoniot may represent a mixture of 'coesite' and stishovite [*Trunin et al.*, 1971*b*]. This point will be discussed further below.

The calculated Hugoniots shown in Figure 1 (stishovite case 2 and 'coesite' case 1, discussed below) reproduce these features fairly well. However, the coesite-stishovite transition is not predicted by these calculations. Thus stishovite Hugoniots corresponding to all seven initial porosities are shown. The three most porous Hugoniots are notable for having negative slopes; there is a critical initial density for which the Hugoniot is vertical. The two most porous Hugoniots are shown as dashed lines, since they clearly fail to represent the corresponding data. The $\rho_0' = 1.55$ Hugoniot data approach but do not agree very well with the corresponding calculated stishovite curve shown in Figure 1. Only the two most porous 'coesite' Hugoniots are shown. The other Hugoniots will lie between these Hugoniots and the 300°K isotherm (shown as a short-dashed line) and clearly will not coincide with the corresponding data.

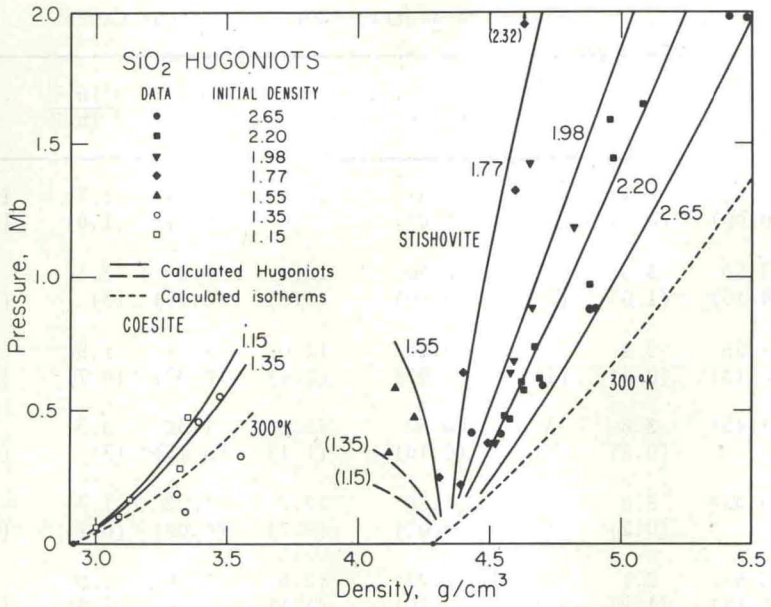

Fig. 1. Hugoniot data of quartz and porous quartz and calculated Hugoniots and 300°K isotherms of 'coesite' and stishovite. Data sources are given in Tables 1 and 2. Calculated curves are from stishovite case 2 (Table 4) and 'coesite' case 1 (Table 6). Numbers labeling curves indicate the initial density of the shocked sample.

The details of the analyses will now be discussed individually for stishovite and 'coesite,' and the effects of assumptions made in the analyses will be noted. However, it will be seen that the preceding general picture is not greatly perturbed.

Stishovite. The results of three different analyses of the stishovite data will now be given. In the first case, standard errors of the pressure of each set of compression data (shock and static) were estimated, and the data were weighted accordingly. (The quantity minimized was $\sum(P_i^c - P_i)^2/\sigma_i^2$, where P_i^c is the calculated pressure, P_i is the observed pressure, σ_i is the estimated standard error, and the summation is over all data points [e.g., *Mathews and Walker*, 1965].) Although K_0 is known approximately from the ultrasonic measurements of *Mizutani et al.* [1972], we preferred to determine it independently from the compression data. Thus the quantities K_0, K_0', K_0'', and $(\partial K/\partial T)_P$ were determined from the compression data, V_0 and α were taken from Table 1, and C_v was calculated from the Debye model. For the calculation of C_v, the Debye temperature given by *Kieffer and Kamb* [1972] as the high temperature limit of the data of *Holm et al.* [1967] was used. The estimated standard errors are listed in Table 3, the resulting values of the parameters and their calculated standard errors are listed in Table 4 (case 1), and the calculated Hugoniots and the 300°K isotherms are compared with the Hugoniot data in Figure 2. It can be seen that this solution does not fit the Hugoniots of the more porous samples

TABLE 3. Standard Errors Assumed for Stishovite Compression Data (All values in megabars.)

Data	Cases 1, 2, and 4	Cases 3 and 5
S1	0.3	0.5
S2	0.2	0.2
S3	0.2	0.1
S4	0.3	0.5
S5	0.3	0.5
S6	0.6	1.0
S7	0.3	0.3
S8	1.0	0.5
S9	1.0	0.1
S10	1.0	1.0
X1	0.015	0.015
X2	0.015	0.015

TABLE 4. Stishovite Parameters Found in Various Cases

Case	K_0, Mb	K_0'	K_0K_0''	$(\partial K_0/\partial T)_P$, kb/°K	α, 10^{-6}/°K	γ_0	$\frac{d \ln \gamma}{d \ln V}$	δ_T
1	3.42 (0.09)	4.9 (0.7)	-2 (5)	-0.61 (0.07)	16.4*	1.61 (0.1)	5.7 (1.6)	10.9 (1.6)
2	3.50 (0.15)	3.5 (1.0)	-2 (3)	-0.30 (0.10)	12.9 (1.3)	1.30 (0.15)	3.1 (3)	6.7 (3)
3	3.55 (0.13)	2.8 (0.4)	-2 (1)	-0.20 (0.03)	12.0 (0.5)	1.22 (0.07)	1.9 (0.7)	4.7 (0.7)
4	3.45*	3.8 (0.8)	-3 (3)	-0.32 (0.10)	13.3 (1.1)	1.32 (0.15)	3.3 (3)	7.1 (3)
5	3.45*	3.0 (0.2)	-2 (1)	-0.20 (0.02)	12.2 (0.2)	1.22 (0.09)	1.7 (0.7)	4.7 (0.7)
2a	3.57 (0.19)	2.1 (1.8)	27 (20)	-0.23 (0.10)	12.6 (1.1)	1.30 (0.14)	2.9 (2.5)	5.0 (2)
3a	3.50 (0.16)	2.2 (1.0)	14 (10)	-0.17 (0.05)	12.1 (0.6)	1.22 (0.08)	1.8 (1)	4.0 (1)

Standard errors due to scatter in the data are given in parentheses.
*Fixed value from Table 1.

very well at all, partly because the data points on the lower-porosity Hugoniots have a greater density and partly because the value of γ_0 is constrained to a high value by the value of α used and the value of K_0 required to fit the lower-porosity Hugoniots.

As a first step toward improving the fit of the higher-porosity Hugoniots, α was allowed to be determined by the compression data, along with the other parameters previously determined. The results are given in Table 4 (case 2) and illustrated in Figure 1, the stishovite curves being those corresponding to the present case. Lowering the value of α to 13×10^{-6}/°K has lowered γ_0 to 1.3 and significantly improved the fit to the higher-porosity Hugoniots. However, the full range of the Hugoniot data is not shown in Figures 1 and 2. The data of *Trunin et al.* [1971*a*, *b*] extending up to 6.5 Mb for the initial densities of 1.77 and 2.65 g/cm³ are shown in Figure 3. The corresponding calculated Hugoniots and the 300°K isotherm of the present case are also shown (case 2). The 1.77-g/cm³ Hugoniot curve does not fit the corresponding datum at 2.3 Mb very well.

To further improve the fit to the higher-porosity Hugoniots, the Hugoniot data were assigned new standard errors to weight the porous data more heavily relative to the other data. The new set of standard errors is given in Table 3. The results are given in Table 4 (case 3) and illustrated in Figures 3 and 4. Figure 3 in particular shows that the fit to the 1.77-g/cm³ Hugoniot data has improved. The value of α has decreased further to 12×10^{-6}/°K.

The values of the zero pressure bulk modulus K_0 range from 3.42 to 3.55 Mb for the three cases considered. These values fall within the range 3.46 ± 0.24 Mb given by *Mizutani et al.* [1972] for the isentropic bulk modulus determined from elastic-wave velocity measurements. The 300°K isotherms for these cases also agree well with the static-compression data of *Liu et al.* [1972]. These data are shown in Figure 5, together with the three calculated isotherms. Also shown are the static-compression data of *Bassett and Barnett* [1970]. These data have been discussed by *Liu et al.* [1972], who suggest that the five highest-pressure data points

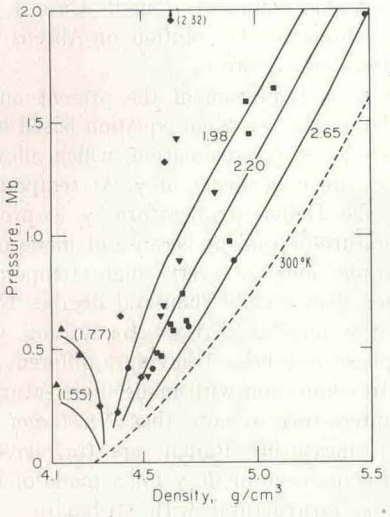

Fig. 2. Hugoniot data of stishovite and calculated Hugoniots and 300°K isotherms from case 1 (Table 4). Symbols are those used in Figure 1.

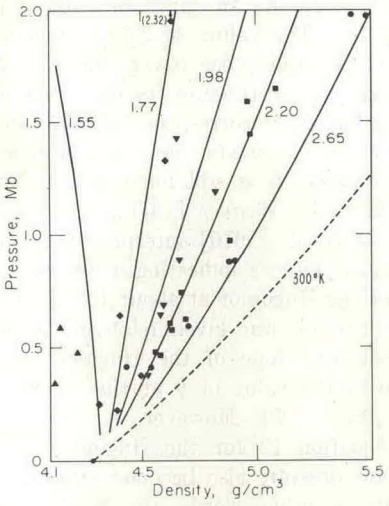

Fig. 4. Hugoniot data of stishovite and calculated Hugoniots and 300°K isotherm from case 3 (Table 4). Symbols are those used in Figure 1.

are systematically low because the anvils of the tetrahedral press used by Bassett and Barnett may have come into contact at about this pressure. These points were not used in the present analysis. The calculated isotherms agree with the remaining data within the scatter of the data.

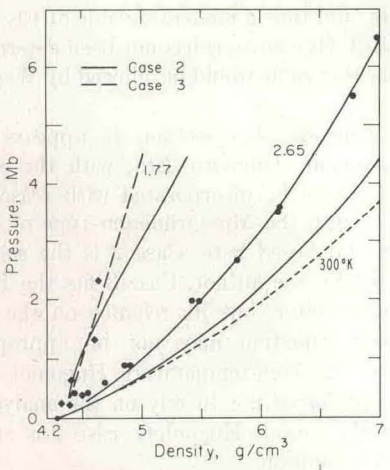

Fig. 3. Very high-pressure Hugoniot data of stishovite and calculated Hugoniots and isotherms from case 2 (solid line) and case 3 (dashed line). Only the Hugoniots corresponding to initial densities 2.65 and 1.77 g/cm³ are shown. Symbols are those used in Figure 1.

The last two cases were rerun with K_0 given the fixed value of 3.45 Mb, which gives an isentropic bulk modulus very close to that given by *Mizutani et al.* [1972]. (In all cases given here, the isentropic bulk modulus is about 0.02 Mb greater than the isothermal bulk modulus.) The results are given in Table 4 (cases 4 and 5). The changes from the previous solutions are small. The standard errors are calculated with the 0.24-Mb error given by Mizutani et al. for the bulk modulus.

In view of the current discussion of the relative merits of the Lagrangian and Eulerian formulations of finite strain [*Thomsen,* 1970, 1972; G. F. Davies, unpublished manuscripts, 1972], the dependence of the preceding results on the form of the equation of state should be tested. This testing was done by using a Lagrangian isotherm [*Thomsen,* 1970; G. F. Davies, unpublished manuscript, 1972] but keeping (5) for γ. This formulation does not correspond to the Lagrangian equation used by *Thomsen* [1970], who used a different expression for γ. This formulation has been discussed previously (G. F. Davies, unpublished manuscript, 1972). In any case, using a different equation for γ should yield a significantly different value for $(\partial K/\partial T)_P$ only, for which we have no other control. Cases 2 and 3 were repeated with the Lagrangian iso-

therm. The results are given in Table 4 (cases 2*a* and 3*a*). The values of K_0 are comparable, those of K_0' somewhat lower, those of K_0K_0'' much higher, and those of the other parameters comparable to the corresponding values in cases 2 and 3. In particular, the value of α is very little changed; it is still much lower than the value given by *Weaver* [1971].

Ahrens et al. [1970] interpreted the $\rho_0' = 1.98$ g/cm³ data as indicating a reversal in the slope of the Hugoniot at about 1.2 Mb (Figure 1). A criterion was given relating the density at which the slope of the Hugoniot becomes infinite to the value of γ at that point: $\gamma = 2/[(\rho/\rho_0') - 1]$. However, it can be seen from equation 12 for the Hugoniot that the Hugoniot pressure also becomes infinite at this density; in other words, the Hugoniot pressure asymptotes to infinity rather than 'bends over.' This interpretation biased the high-pressure values of γ to lower values, since it favored an interpretation in which the Hugoniots were crowded together at these compressions. The discrepancy between the results of *Ahrens et al.* [1970] and those of this study is due partly to the last effect, partly to the fewer data available at the time, and partly to the higher value of α used. Case 1 given here is closer to the solution of Ahrens et al. and shows similar effects.

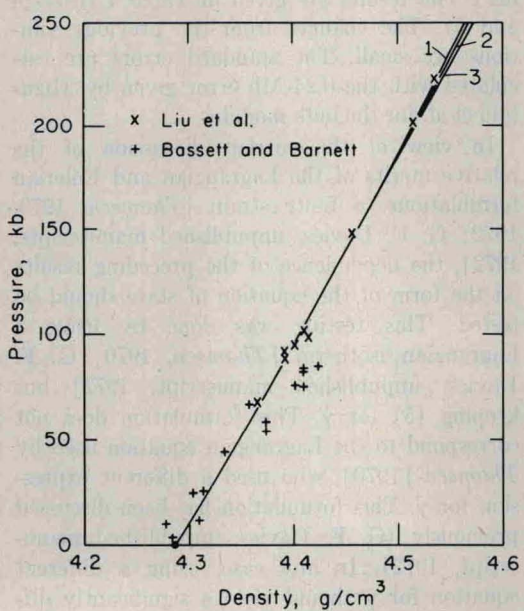

Fig. 5. Static-compression data of stishovite compared with 300°K isotherms calculated from cases 1, 2, and 3.

The main limitation of the present analysis is probably the use of an equation based on the Mie-Grüneisen approximation, which allows no temperature dependence of γ. At temperatures below the Debye temperature, γ is probably temperature-dependent because of mode undersaturation, and, at very high temperatures (greater than several thousand degrees Kelvin, say), it is possible that we are dealing with a fluid phase (see below) having a different value of γ. In connection with mode undersaturation, it is interesting to note that *Nicol and Fong* [1971], measuring Raman spectra, have observed a negative mode γ for a mode of rutile, which is isostructural with stishovite.

The temperature dependence of α is dominated by the temperature dependence of C_p and possibly of γ (see equation 2). *Weaver* [1971] notes that his value of $\epsilon = (\partial\alpha/\partial T)_p/\alpha^2 = 33 \pm 17$ seems too small; it implies that $(\partial\gamma/\partial T)_v = -5 \times 10^{-3}$/°K, a value sufficient to reduce γ to zero within 300°K. With $(\partial\gamma/\partial T)_v = 0$, Weaver estimates that $\epsilon = 190 \pm 20$. If we take Weaver's mean value of α in the range 300°–900°K (i.e., $\alpha = 18.6 \times 10^{-6}$/°K) to apply to 600°K and combine it with the 300°K value of 13×10^{-6}/°K found here, we get $\epsilon = 100$ approximately. This value is intermediate, and thus a moderate value of $(\partial\gamma/\partial T)_v$ is implied. Of course, it has not been determined whether this value would be allowed by Weaver's data.

To conclude this section, it appears that most relevant stishovite data, with the exception of α, can be incorporated with reasonable accuracy into the Mie-Grüneisen–type of equation of state used here. Case 2 is the solution preferred by the author. Case 3 fits the Hugoniot data better, but its reliance on the Mie-Grüneisen equation may not be appropriate for the very high-temperature Hugoniot data. If it is preferred not to rely on the analysis of any of the porous Hugoniots, case 1 is an appropriate solution.

'Coesite.' This section will assume that the Hugoniots of the most porous quartz samples represent coesite. The difficulties raised by this assumption and an alternative interpretation will be discussed in the next section.

Because of the smaller range and quantity of 'coesite' data, it is not possible to determine as many parameters of the equation of state as were determined for the stishovite data. Because the data extend to only about 15% volume compression, it is not necessary to use the full fourth-order version of (3), and so the ϵ^3 term is here assumed to be zero. Because there is not a large range in the initial porosities of the Hugoniot data, the volume dependence of γ, and hence $(\partial K/\partial T)_P$, cannot be well determined. Conversely, the value of $(\partial K/\partial T)_P$ does not strongly affect the equation of state in this range. A value of -0.05 kb/°K was therefore assumed. This value of $(\partial K/\partial T)_P$ gives values of δ_T in the range 5–10, a range that seems reasonable on the basis of a few other examples, including stishovite [e.g., *Anderson et al.*, 1968; *Roberts and Ruppin*, 1971]. The values of V_0 and α were taken from Table 2, and C_v was calculated from the Debye model.

It can be seen from Figure 1 that the $\rho_0' = 1.35$ g/cm³ Hugoniot data are considerably scattered and that they do not trend toward the coesite density of 2.91 g/cm³, perhaps because there has been a partial conversion to the stishovite phase. When they are compared to the $\rho_0' = 1.15$ g/cm³ Hugoniot data, the lower three points in particular are seen to deviate toward higher densities. Two cases were therefore treated, one including these three points, the other excluding them.

Initially both K_0 and K_0' were determined by the Hugoniot and static-compression data. The results are given as cases 1 and 2 in Table 6, case 1 excluding the three doubtful Hugoniot points and case 2 including them. The standard errors used to weight the compression data are given in Table 5. Case 1 is illustrated in Figure 1, case 2 in Figure 6. The bulk moduli in these two cases are significantly above the value of 0.97 Mb measured ultrasonically by Mizutani et al. (H. Mizutani, private communication, 1972), and so a third case was run with K_0 fixed at this value and only K_0' determined by the compression data (Table 6 and Figure 6). It can be seen (Figure 6) that case 3 does not fit the static-compression data of *Bassett and Barnett* [1970] very well, and it falls below most of the corresponding Hugoniot data.

The scatter in the Hugoniot data and the uncertainty in their interpretation are such that they cannot definitely be said to be discordant with case 3, but the discrepancy between case 3 and the static-compression data seems to be significant. Because of this discrepancy, the equation of state of coesite must remain somewhat uncertain at this stage.

TABLE 5. Standard Errors Assumed for the 'Coesite' Compression Data

Data	Error, Mb
S11	0.20
S12	0.10
S13	0.10
X3	0.02

SiO_2 PHASE EQUILIBRIA

By using the equations of state just given, the Gibbs free energies of 'coesite' and stishovite can now be calculated, and the 'coesite'-stishovite transition pressure can be calculated as a function of temperature by using the condition that the Gibbs free energies of the two phases are equal at the phase transition.

For detailed comparison the Hugoniot temperatures, which were calculated approximately by *Trunin et al.* [1971*b*], have been calculated according to the method described earlier. The results are plotted against Hugoniot pressure (Figures 7 and 8). It is notable that the 5.5-Mb point is over 40,000°K and that the $\rho_0' = 1.77$ point at 2.3 Mb is over 30,000°K. The temperatures are changed by only a few per cent by using the different equations of state given in the previous sections. A greater uncertainty in the points is due to the scatter in Hugoniot pressures, but this scatter would only cause

TABLE 6. 'Coesite' Parameters for Various Cases

Case	K_0, Mb	K_0'	$(\partial K_0/\partial T)_P$*	γ	$\frac{d \ln \gamma}{d \ln V}$	δ_T
1	1.27	5.6	-0.05	0.43	-0.04	4.9
2	1.36	4.1	-0.05	0.46	1.2	4.6
3	0.97†	7.3	-0.05	0.33	-0.15	6.4

*Assumed values (see text).
†Fixed value from Table 2.

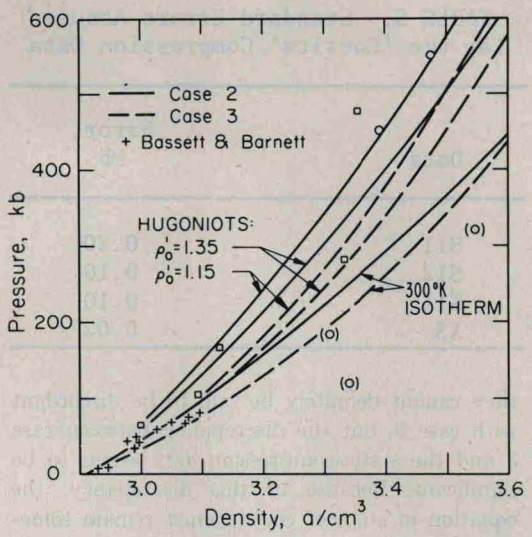

Fig. 6. Hugoniot data of 'coesite' and calculated Hugoniots and 300°K isotherms from cases 2 and 3 (Table 6). Symbols are those used in Figures 1 and 5.

the points to move along the Hugoniot locus, which in a P-T plot is approximately radial from the initial point.

The boundary between the 'coesite' and stishovite fields (Figure 8) is closely defined by the $\rho_0' = 1.77$ and $\rho_0' = 1.55$ g/cm^3 Hugoniot points, both of which show signs involving a mixture of the two phases, as was discussed earlier.

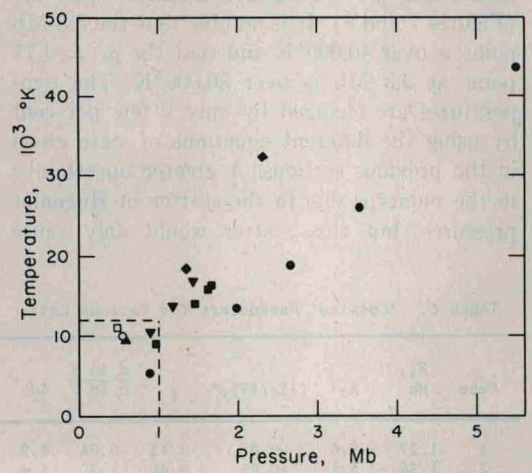

Fig. 7. Calculated Hugoniot temperatures of stishovite and 'coesite' versus Hugoniot pressure. Box is enlarged in Figure 8. Symbols are those used in Figure 1.

The Gibbs free energy is defined by

$$G = H - TS = U + PV - TS \qquad (14)$$

where H is the enthalpy and S is the entropy. Here G has the property [e.g., *Slater*, 1939]

$$(\partial G/\partial P)_T = V \qquad (15)$$

We wish to evaluate G at the state (P, V, T), starting from the state (O, V_0, T_0). (Atmospheric pressure can be ignored here.) This evaluation will be done via the state (P_0, V_0, T), where $P_0(T) = P(V_0, T)$ (i.e., by first raising the temperature at constant volume and then compressing isothermally). From (14)

$$G(V_0, T) = G(V_0, T_0) + [U(V_0, T) - U(V_0, T_0)] + P_0(T)\,V_0 - [TS(V_0, T) - T_0 S(V_0, T_0)] \qquad (16)$$

and from (15), upon integration,

$$G(V, T) = G(V_0, T) + \int_{P_0(T)}^{P(T)} V(P', T)\, dP' \qquad (17)$$

When the difference between the Gibbs free energies of stishovite and coesite at the state (V_0, T_0) are denoted by ΔG_0 (i.e.,

$$\Delta G_0 = G^s(V_0{}^s, T_0) - G^c(V_0{}^c, T_0)$$

where superscripts s and c denote stishovite and

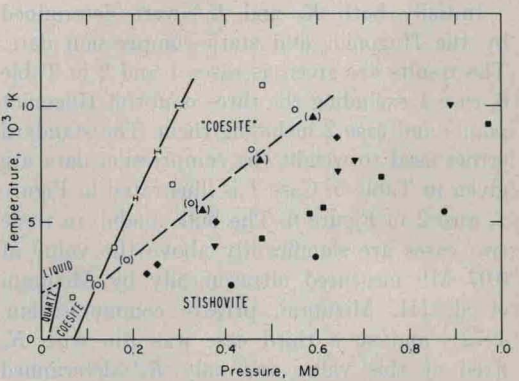

Fig. 8. Calculated Hugoniot temperatures of stishovite and 'coesite' versus Hugoniot pressure compared with observed and calculated (solid and short-dashed) phase lines. Long-dashed line separates stishovite and 'coesite' fields. Error bars represent variations due to the use of alternative equations of state given in previous sections. Symbols are those used in Figure 1.

coesite, respectively) and ΔH_0 and ΔS_0 are defined similarly, (14) gives

$$\Delta G_0 = \Delta H_0 - T_0 \Delta S_0 \qquad (18)$$

The values of ΔH_0 and ΔS_0 can be found from the results of *Holm et al.* [1967]. At 298°K $\Delta H_0 = 10.58$ kcal/mole $= 7.36 \times 10^9$ ergs/g and $\Delta S_0 = -3.01$ cal/mole°K $= -2.09 \times 10^8$ ergs/g°K.

Now from (16), using (18), we obtain

$$G^s(V_0^s, T) - G^c(V_0^c, T) = P_0(T)(V_0^s - V_0^c) + U^s(V_0^s, T) - U^c(V_0^c, T) - T[S^s(V_0^s, T) - S^c(V_0^c, T)] \qquad (19)$$

To evaluate this expression we need U and S as functions of T for both stishovite and coesite. These functions are known accurately [*Holm et al.*, 1967] only up to 350°K. However, the difference $U^s(V_0^s, T) - U^c(V_0^c, T)$ and the analogous difference for S can be approximated as being constant above about 350°K for the following reasons. The specific heats C_p of stishovite and coesite given by *Holm et al.* [1967] converge toward each other above about 150°K. Also, at 300°K, C_p differs from C_v by about 0.6% for stishovite and by about 0.1% for coesite. Thus the C_v will also converge at higher temperatures. Because U and S are integrals of C_v, $U^s - U^c$ will approach a constant value at higher temperatures, as will $S^s - S^c$. Thus the differences in U and S in (19) can be replaced by their values at 298°K. When it is noted, finally, that $\Delta U_0 \approx \Delta H_0$, (19) becomes

$$G^s(V_0^s, T) - G^c(V_0^c, T) = P_0(V_0^s - V_0^c) + \Delta H_0 - T\Delta S_0 \qquad (20)$$

The integral in (17) is more easily evaluated here by noting that

$$\int_{P_0}^{P} V\, dP' = \int_{V}^{V_0} P(V', T)\, dV' + VP - V_0P_0 \qquad (21)$$

Equations 17, 20, and 21 and equation 3 for an isotherm allow the Gibbs free energies of 'coesite' and stishovite to be compared.

The phase line resulting from these calculations is shown in Figure 8. The error bars represent variations due to the use of the alternative equations of state given in the previous sections. The uncertainty due to the approximations used for $U^s - U^c$ and $S^s - S^c$ is difficult to estimate, but it should not be greater than a few per cent. Errors of 5% in $U^s - U^c$ and $S^s - S^c$ would cause errors of about 1 and 3%, respectively, in the calculated transition pressure at 10,000°K.

As can be seen in Figure 8, the calculated phase line deviates considerably from the line separating the 'coesite' and stishovite Hugoniot fields. The difference is about a factor of 2 in temperature, which would seem to be well outside the range of uncertainties of the calculations. If this result is correct, the phase obtained in the shock-wave experiments is outside the coesite stability field. It would be surprising if this phase were coesite, since it would be expected that the high temperatures involved would promote the transition to stishovite.

An alternative interpretation of the data is suggested by re-examining Figure 8, in which the lower-pressure quartz-liquid-gas region of the phase diagram is also shown [*Levin et al.*, 1969; *JANAF Tables*, 1965]. The 'coesite'-stishovite Hugoniot boundary intersects the calculated phase line at about 2500°K, which is comparable to the melting temperature of quartz. Is it possible that the 'coesite' is the liquid phase?

The plausibility of this hypothesis can be tested by using the Clausius-Clapeyron relation for the slope of a phase line:

$$dP/dT = \Delta S/\Delta V \qquad (22)$$

where Δ denotes the change through the phase transition. Let us apply this at the hypothetical coesite-stishovite-liquid triple point at 125 kb and 2500°K. We know that the volumes of the coesite and the liquid must be very similar at this pressure because of the agreement between the coesite static-compression data and the 'coesite' Hugoniot data (Figure 6). If the difference in their volumes is zero, (22) shows that the coesite-liquid phase line is horizontal in Figure 8 (also shown by line 1 in Figure 9, which illustrates the relevant region of the phase diagram in more detail). If the difference in volumes is not zero, the slope of the phase line can be estimated as follows. The coesite-stishovite phase line is still fairly well determined below the triple point. The coesite-

stishovite volume difference is about 0.09 cm^3/g. The entropy difference is, then, from either the slope of the phase line (0.02 kb/°K) and (22) or the approximation made in the previous section, about 2×10^6 ergs/g°K. When the liquid-stishovite volume difference is assumed to be also about 0.09 cm^3/g, the slope of the liquid-stishovite phase line (0.06 kb/°K) and (22) give the liquid-stishovite entropy difference as about 5×10^6 ergs/g°K. When these results are combined, the liquid-coesite entropy difference is about 3×10^6 ergs/g°K. From Figure 6 we can estimate a reasonable maximum volume difference between the coesite and the liquid to be about 0.01 cm^3/g. Equation 22 then gives a slope of about 0.3 kb/°K (line 2 in Figure 9). Line 3, which has the same slope as the stishovite-liquid phase line, would imply that coesite has a volume similar to that of stishovite, which is clearly unreasonable.

Lines 1 and 2 both extrapolate to the range of melting temperatures of quartz. There is a difficulty, though, since a similar set of relationships would hold at the quartz-coesite-liquid triple point, and thus we would be led to predict a slope of the quartz-liquid phase line rather different from the one shown. However, we may observe that the liquid would have to vary continuously from a density of about 2.2 g/cm^3 at zero pressure (the density of fused quartz) to about 3.1 g/cm^3 at 100 kb. This variation would cause the phase lines to be concave downwards (Figure 9) in this range and might allow these relationships to hold without contradiction.

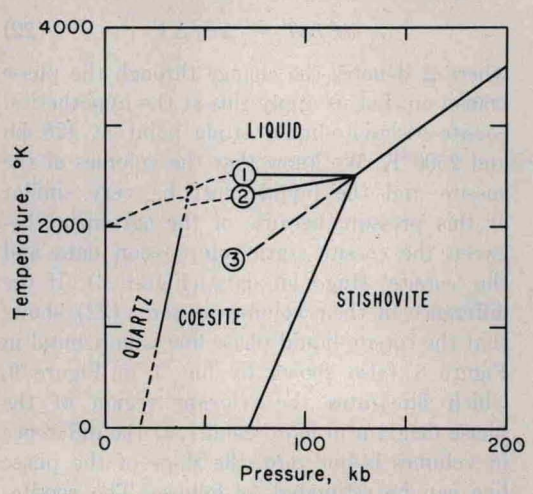

Fig. 9. Hypothetical silica phase diagram. Lines 1, 2, and 3 correspond to different assumptions about the relative densities of the coesite and the liquid (see text).

The preceding discussion is intended as a plausibility argument. It must be considered a serious possibility that a coesitelike liquid phase was produced in the shock-wave experiments.

To return, finally, to the coesite-stishovite phase line below the hypothetical triple point, the calculated transition pressure at 300°K is 78 kb. This value is in reasonable agreement with that of 69 kb estimated by *Akimoto and Syono* [1969] from their experimental results. It may also be compared with their values of 85–95 kb calculated by using a rough estimate of the coesite compressibility.

The average slope of the phase line is about 0.023 kb/°K, which compares very well with the value of 0.024 kb/°K found by *Akimoto and Syono* [1969].

Note added in proof. An analysis by E. K. Graham (unpublished manuscript, 1972) of some of the stishovite Hugoniot data analyzed here yielded the values $K_0 = 3.35$ Mb, $K_0' = 5.5$, and $\gamma_0 = 1.64$. A high value of K_0' was also obtained by *Ahrens et al.* [1970] ($K_0 = 3.0$, $K_0' = 6.9$, $\gamma_0 = 1.58$). Although some differences between these analyses and the present analysis are due to the different equations used, a critical difference is that cases 2 and 3 of the present analysis rely on the Hugoniot data of the more porous samples to constrain γ, whereas those in the other analyses rely on *Weaver's* [1971] coefficient of thermal expansion. The effect of these different approaches can be seen by comparing case 1 with cases 2 and 3 above. Case 1 also relies on Weaver's data. The preference for case 2 rests on the critical assumption that the Grüneisen parameter does not vary greatly with temperature at very high temperatures.

Acknowledgments. I am grateful to Dr. Tom Ahrens for suggestions concerning the calculation of phase equilibria and to Dr. H. Mizutani for providing data in advance of publication.

* * *

This research was supported by National Science Foundation grants GA-12703 and GA-21396.

REFERENCES

Ahrens, T. J., D. L. Anderson, and A. E. Ringwood, Equations of state and crystal structures of high-pressure phases of shocked silicates and oxides, *Rev. Geophys. Space Phys.*, *7*, 667–707, 1969.

Ahrens, T. J., T. Takahashi, and G. F. Davies, A proposed equation of state of stishovite, *J. Geophys. Res., 75,* 310–316, 1970.

Akimoto, S., and Y. Syono, Coesite-stishovite transition, *J. Geophys. Res., 74,* 1653–1659, 1969.

Al'tshuler, L. V., R. F. Trunin, and G. V. Simakov, Shock-wave compression of periclase and quartz and the composition of the earth's lower mantle, *Izv. Acad. Sci. USSR Phys. Solid Earth,* no. 10, 657–660, 1965.

Anderson, D. L., and H. Kanamori, Shock-wave equations of state for rocks and minerals, *J. Geophys. Res., 73,* 6477–6502, 1968.

Anderson, O. L., E. Schreiber, R. C. Liebermann, and N. Soga, Some elastic constant data on minerals relevant to geophysics, *Rev. Geophys. Space Phys., 6,* 491–524, 1968.

Bassett, W. A., and J. D. Barnett, Isothermal compression of stishovite and coesite up to 85 kilobars at room temperature by X-ray diffraction, *Phys. Earth Planet. Interiors, 3,* 54–60, 1970.

Bassett, W. A., T. Takahashi, H. K. Mao, and J. S. Weaver, Pressure-induced phase transformation in NaCl, *J. Appl. Phys., 39,* 319–325, 1968.

Birch, F., Elasticity and constitution of the earth's interior, *J. Geophys. Res., 57,* 227–286, 1952.

Chao, E. C. T., J. J. Fahey, J. Littler, and D. J. Milton, Stishovite, *Amer. Mineral., 46,* 807, 1962.

Dugdale, J. S., and D. K. C. MacDonald, The thermal expansion of solids, *Phys. Rev., 89,* 832–834, 1953.

Holm, J. L., O. J. Kleppa, and E. F. Westrum, Thermodynamics of polymorphic transformations in silica, *Geochim. Cosmochim. Acta, 31,* 2289–2307, 1967.

Joint Army, Navy, and Air Force (JANAF) Thermochemical Tables, Nat. Bur. of Stand., Washington, D.C., 1965. (Also available as *SN 0303-0872,* Govern. Print. Office, Washington, D.C.)

Jones, A. A., W. M. Isbell, F. H. Shipman, R. D. Perkins, S. J. Green, and C. J. Maiden, Material property measurements for selected materials, *Rep. NAS2-3427,* 56 pp., Gen. Mot. Mater. and Struct. Lab., Warren, Mich., 1968.

Kieffer, S. W., and B. Kamb, The specific heats of solids of geophysical interest, *Rev. Geophys. Space Phys., 10,* in press, 1972.

Knopoff, L., and J. N. Shapiro, Comments on the interrelationships between Grüneisen's parameter and shock and isothermal equations of state, *J. Geophys. Res., 74,* 1439–1450, 1969.

Leibfried, G., and W. Ludwig, Theory of anharmonic effects in crystals, *Solid State Phys., 12,* 275–444, 1961.

Levin, E. M., C. R. Robbins, and H. F. McMurdie, *Phase Diagrams for Ceramicists,* 2nd ed., p. 84, American Ceramics Society, Columbus, Ohio, 1969.

Liu, L., W. A. Bassett, and T. Takahashi, Effect of pressure on the lattice parameters of stishovite, *J. Geophys. Res., 77,* this issue, 1972.

Mathews, J., and R. L. Walker, *Mathematical Methods of Physics,* p. 365, W. A. Benjamin, New York, 1965.

McQueen, R. G., Shock-wave data and equation of state, in *Seismic Coupling, VESIAC Report,* edited by G. Simmons, pp. 53–106, Geophys. Lab., Univ. of Mich., Ann Arbor, 1968.

McQueen, R. G., J. N. Fritz, and S. P. Marsh, On the equation of state of stishovite, *J. Geophys. Res., 68,* 2319–2322, 1963.

Mizutani, H., Y. Hamano, and S. Akimoto, Elastic-wave velocities of polycrystalline stishovite, *J. Geophys. Res., 7,* 3744–3749, 1972.

Nicol, M., and N. Y. Fong, Raman spectrum and polymorphism of titanium dioxide at high pressures, *J. Chem. Phys., 54,* 3167–3170, 1971.

Roberts, R. W., and R. Ruppin, Volume dependence of the Grüneisen parameter of alkali halides, *Phys. Rev. B, 4,* 2041–2046, 1971.

Robie, R. A., P. M. Bethke, M. S. Toulmin, and J. L. Edwards, X-ray crystallographic data, densities and molar volume of minerals, in *Handbook of Physical Constants, Mem. 97,* edited by S. P. Clark, Jr., pp. 27–74, Geological Society of America, Boulder, Colo., 1966.

Skinner, B. J., Thermal expansion, in *Handbook of Physical Constants, Mem. 97,* edited by S. P. Clark, Jr., pp. 75–96, Geological Society of America, Boulder, Colo., 1966.

Slater, J. C., *Introduction to Chemical Physics,* p. 22, McGraw-Hill, New York, 1939.

Stishov, S. M., and S. V. Popova, A new dense modification of silica, *Geokhimiya,* no. 10, 923–926, 1961.

Thomsen, L., On the fourth-order anharmonic equation of state of solids, *J. Phys. Chem. Solids, 31,* 2003–2016, 1970.

Thomsen, L., The fourth-order anharmonic theory: Elasticity and stability, *J. Phys. Chem. Solids, 33,* 363–378, 1972.

Trunin, R. F., G. V. Simakov, M. A. Podurets, B. N. Moiseyev, and L. V. Popov, Dynamic compressibility of quartz and quartzite at high pressure, *Izv. Acad. Sci. USSR Phys. Solid Earth,* no. 1, 13–20, 1971*a*.

Trunin, R. F., G. V. Simakov, and M. A. Podurets, Compression of porous quartz by strong shock waves, *Izv. Acad. Sci. USSR Phys. Solid Earth,* no. 2, 33–39, 1971*b*.

Wackerle, J., Shock-wave compression of quartz, *J. Appl. Phys., 33,* 922–937, 1962.

Weaver, J. S., Equation of state of NaCl, MgO, and stishovite, Ph.D. thesis, 173 pp., Univ. of Rochester, Rochester, N.Y., 1971.

(Received December 8, 1971;
revised May 4, 1972.)